Acta Cryst. (1974). A30, 662

Debye–Waller Coefficient of KCl by the Powder Neutron Diffraction Method

BY M. M. BEG, J. ASLAM, N. M. BUTT, Q. H. KHAN AND S. ROLANDSON*

Pakistan Institute of Nuclear Science & Technology, P.O. Nilore, Rawalpindi, Pakistan

(*Received* 22 *March* 1974; *accepted* 16 *April* 1974)

The neutron diffraction pattern of powdered KCl has been measured using the triple-axis spectrometer both in the double-axis and the triple-axis modes. The thermal diffuse scattering (TDS) correction, which is very important in the double-axis pattern, is essentially eliminated in the triple-axis mode. Theoretical calculations are presented which give the relative TDS correction for the two cases by calculating the energy distribution of TDS. The Debye–Waller coefficient B using the triple-axis data is found to be ($2{\cdot}17 \pm 0{\cdot}16$ Å^2), which is in agreement with the TDS-corrected values of other workers.

1. Introduction

The Debye–Waller coefficient B for KCl has been obtained by many workers using X-ray diffraction (James & Brindley, 1928; Patomaki & Linkoaho, 1968; Jayalakshmi & Viswamitra, 1970), Mössbauer γ-ray diffraction (Butt & O'Connor, 1967) and neutron diffraction techniques (Cooper & Rouse, 1973). The B values have also been calculated theoretically from various lattice-dynamical models (Copley, Macpherson & Timusk, 1969; Reid & Smith, 1970; Groenewegen & Huiszoon, 1972).

The experimental B values reported since 1967 (Butt & O'Connor) are in general agreement with one another. However, the theoretical values are smaller than the experimental values. In the X-ray and neutron diffraction methods, the coefficient B is evaluated from the angular dependence of the intensity of Bragg reflexions. The intensities of the diffraction peaks are not purely due to elastic scattering and contain the thermal diffuse scattering (TDS). The observed Bragg intensities are corrected for the TDS evaluated theoretically or experimentally. The corrected intensities are then used to obtain the coefficient B.

In the case of X-ray and double-axis neutron diffraction from single crystals the TDS originates from phonons of very small energies, from a small volume around the reciprocal-lattice point defined by the experimental collimation (Nilsson, 1957; Willis, 1969). For single crystals the TDS can however be eliminated experimentally by the Mössbauer technique. Theoretical calculations have been performed which show that the TDS in powder samples has a large contribution from phonons of energies greater than the energy resolution of the triple-axis neutron spectrometer. Hence this technique has been used to reduce the TDS considerably, and to determine the B values accurately.

* Permanent Address: AB Atomenergi, Studsvik, Sweden.

2. Experimental procedure

The triple-axis neutron spectrometer TKSN-400 at the PINSTECH 5 MW research reactor was used to measure the double-axis and the triple-axis powder diffraction patterns. KCl powder (AnalaR grade) was packed in a moisture-tight rectangular container of size $11 \times 5 \times 0{\cdot}5$ cm with thin aluminum walls. The sample thickness corresponded to a 76% neutron transmission at the wavelength 1·18 Å, used in the experiment. Zn (0002) single crystals were used as monochromator and analyzer. The Soller collimators used before and after the sample were 20′ and 30′ respectively.

The observed integrated intensity P_{hkl} for the Bragg peak hkl is given by (Bacon, 1962)

$$P_{hkl} = A \, . \, C_{hkl} \exp(-2B \sin^2\theta/\lambda^2) \qquad (2.1)$$

where A is a constant for the apparatus,

$$C_{hkl} = \frac{\exp(-\mu t \sec\theta)}{L(\theta)} j_{hkl} F_{hkl}^2 ,$$

j_{hkl} the multiplicity of the planes of reflexion, F_{hkl} the structure factor, θ the Bragg angle, μ the linear absorption coefficient of the sample, t the thickness of the sample and $L(\theta)$ the Lorentz factor, which for a slab sample is $1/\sin^2 2\theta$.

The integrated intensities P_{hkl} of the diffraction peaks were measured by planimetry by taking the area above the background defined by the wings of the peaks. The quantities C_{hkl} were calculated theoretically for each peak, and the coefficient B was found from equation (2.1). A computer program was written for the calculation of C_{hkl} and for the evaluation of B along with the error on it. The neutron scattering amplitudes used for K and Cl were $0{\cdot}369 \times 10^{-12}$ and $0{\cdot}958 \times 10^{-12}$ cm respectively (Willis, 1973). All measurements were made at room temperature.

3. TDS Calculations

The thermal diffuse scattering (TDS) originates from phonon coherent scattering. In the case of neutrons the one-phonon processes are most important and are governed by the following wave vector and energy conditions:

$$\mathbf{K}_1-\mathbf{K}_2=\boldsymbol{\tau}+\mathbf{q} \tag{3.1}$$

$$\frac{\hbar^2K_1^2}{2m}-\frac{\hbar^2K_2^2}{2m}=\pm\hbar\omega(\mathbf{q})\,. \tag{3.2}$$

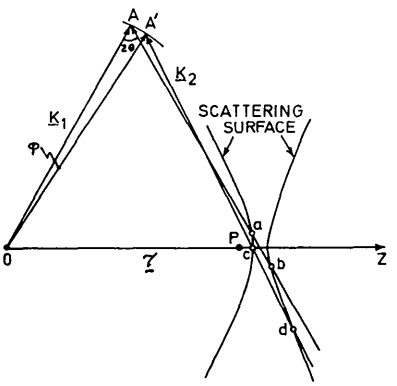

Fig. 1. Scattering surfaces for powder sample. These are generated when the configuration $\mathbf{K}_1$, $\mathbf{K}_2$ is rotated in reciprocal space keeping 2θ fixed. A and A' show two positions of $\mathbf{K}_1$ during rotation. The wave vector $\mathbf{K}_2$ intersects the scattering surfaces at a, b and c, d in the two cases. The distance of these points from the reciprocal point P gives the q value of the phonons involved in the scattering process.

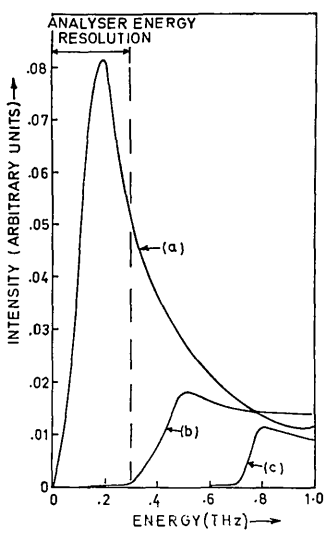

Fig. 2. Energy distribution of thermal diffuse scattering for the Bragg peak 420. The contribution from energy gain and energy loss processes are added together. Curves (*a*), (*b*) and (*c*) give the energy distribution at three different angular positions (within the Bragg peak) at a distance δ, 3δ and 6δ away from the Bragg angle. δ is 1/20th of the full base width of the peak.

$\mathbf{K}_1$ and $\mathbf{K}_2$ are the wave vectors of the incoming and outgoing neutrons respectively, $\boldsymbol{\tau}$ a reciprocal-lattice vector, m the neutron mass, $\mathbf{q}$ the wave vector and $\omega(\mathbf{q})$ the frequency of the phonon taking part in the scattering.

The scattering surfaces for TDS in the single crystal case were first given by Seeger & Teller (1942). They showed that by varying the scattering angle the solutions to equations (3.1) and (3.2) could be represented by a quadratic surface in reciprocal space under the assumption that $\omega(q)=cq$ and $q\ll\tau$ where c is an effective velocity of sound. This limits the validity of the treatment to a small region around the reciprocal-lattice point. The scattering surface is a hyperboloid if $K_1<c/m$ and an ellipsoid if $K_1>c/m$, the axis of symmetry being the wave vector $\mathbf{K}_2$ at the Bragg angle (Willis, 1969).

To obtain the TDS for a powder sample, which contains a large number of crystallites with random orientation, we have to take an average over all directions. This can be done by rotating the reciprocal lattice in the scattering diagram such that each point generates a spherical surface or, alternatively, by keeping the reciprocal lattice fixed and rotating $\mathbf{K}_1$ and $\mathbf{K}_2$, with a constant scattering angle. The latter picture is illustrated in Fig. 1. Using the same assumptions as Seeger & Teller the solution to equations (3.1) and (3.2) generates the following scattering surface for the powder case (Appendix)

$$\frac{(1-d)}{d}\left(z-\frac{\Delta}{1-d}\right)^2-r^2-\frac{\Delta^2}{1-d}=0 \tag{3.3}$$

where z and r are cylindrical coordinates with z in the direction of $\boldsymbol{\tau}$ and

$$d=\frac{m^2\tau c^2}{4\hbar^2K_1^4}$$

$$\Delta=2K_1\sin\theta-\tau\,.$$

For $d>1$ equation (3.3) represents an ellipsoid and for $d<1$ a hyperboloid.

The scattering surface for the case $d<1$ is shown in Fig. 1. In both cases $\boldsymbol{\tau}$ is a symmetry axis and the symmetry centre is $\Delta/(1-d)$ away from the reciprocal-lattice point. For the ellipsoid case the reciprocal-lattice point is within the ellipsoid and for the hyperboloid case the two branches are on the same side of the lattice point.

To obtain a value for the parameter c which is an effective sound velocity of the material, we used the sum

$$S_q=\sum_{j=1}^{3}\frac{\cos^2\alpha_j(q)}{\varrho V_{q,j}^2} \tag{3.4}$$

where $\alpha_j(q)$ is the angle between a fixed direction and the polarization of mode (q,j), $V_{q,j}$ the corresponding sound velocity and ϱ the density. Nilsson (1957) has

shown that in the isotropic approximation a value of S_q is obtained by

$$S=\frac{1}{3}\frac{\frac{1}{5}b_1(c_{11}+c_{12})+c_{44}(2c_{11}+c_{44})}{\frac{1}{105}b_1^2b_2+\frac{1}{5}b_1(c_{11}+c_{12})c_{44}+c_1c_{44}^2} \quad (3.5)$$

where

$$b_1=(c_{11}-c_{12}-2c_{44})$$
$$b_2=(c_{11}+2c_{12}+c_{44})\,.$$

As $\langle\cos^2\alpha_j(q)\rangle=\frac{1}{3}$ we obtain by averaging the numerator and the denominator separately in equation (3.4)

$$\langle S_q\rangle=\sum_{j=1}^{3}\frac{\frac{1}{3}}{\varrho\langle V_q^2\rangle_j}\,. \quad (3.6)$$

Let the effective sound velocity c be given by

$$\frac{1}{c^2}=\frac{1}{3}\sum_{j=1}^{3}\frac{1}{\langle V_q^2\rangle_j}\,. \quad (3.7)$$

From equations (3.5), (3.6) and (3.7) we finally obtain.

$$c=(\varrho\,.\,S)^{-1/2}\,.$$

The one-phonon coherent cross section in the high-temperature limit is

$$\sigma=\frac{N|F(Q)|^2}{m}\,Q^2k_BT\sum_{j=1}^{3}\frac{\cos^2\alpha_j(q)}{\omega_{q,j}^2} \quad (3.8)$$

where N is the number of unit cells in the crystal, $F(Q)$ the structure factor, and $\alpha_j(q)$ the angle between the direction of polarization of the mode (q,j) and the scattering vector $\mathbf{Q}$ given by

$$\mathbf{Q}=\boldsymbol{\tau}+\mathbf{q}\,.$$

Using relations (3.4) and (3.8) we obtain

$$\sigma=\frac{N|F(\mathrm{Q})|^2}{v_c}\,k_BTS_q\,\frac{1}{q^2}$$

where v_c is the volume of the unit cell.

By integrating this scattering cross section over the scattering surface the total TDS for a specific scattering angle can be obtained.

The TDS of interest is the peaked contribution under the elastic peaks and this originates from a limited region in the Brillouin zone of the particular reciprocal-lattice point. The contributions from other parts of the scattering surface only give rise to a slowly varying background. Therefore we only perform the integration over that part of the scattering surface which lies within the first Brillouin zone. A computer program was written to calculate the relative TDS from this model for the double-axis and the triple-axis cases. The observed base width of the double-axis peaks was divided into 20 steps and the energy distribution of the TDS was calculated for each step (Fig. 2). In the double-axis mode, this energy distribution is integrated to give the TDS contribution for each step. Since we are only interested in the peaked TDS contribution, the constant contribution, defined as the TDS value at peak edges, was treated as background and subtracted to give the net TDS contribution. The total TDS correction for the peak was taken to be the sum of these 20 contributions.

4. Results and discussion

The double-axis neutron diffraction pattern of KCl is shown in Fig. 3. In this pattern the background goes up with angle indicating the presence of large incoherent inelastic scattering. This follows from the fact that the one-phonon incoherent scattering cross section goes up as $\sin^2\theta/\lambda^2\,.\,\exp(-2B\sin^2\theta/\lambda^2)$ whereas the incoherent elastic scattering goes down as $\exp(-2B\sin^2\theta/\lambda^2)$. The rising background includes the incoherent inelastic scattering and the coherent inelastic scattering, which, outside the region of Bragg peaks, can be treated like incoherent inelastic scattering for powder samples (Beg & Ross, 1968; Roy & Brockhouse, 1970; Gompf, Lau, Reichardt & Salgado, 1972). The presence of large inelastic scattering suggests a sizable TDS under the Bragg peaks.

The average B value for KCl, without TDS correction obtained from the double-axis pattern is

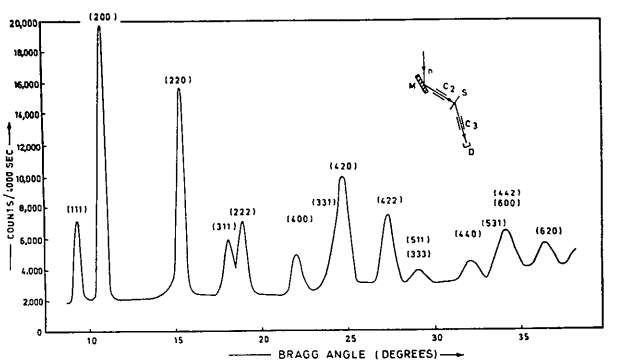

Fig. 3. Double-axis neutron diffraction pattern of KCl powder.

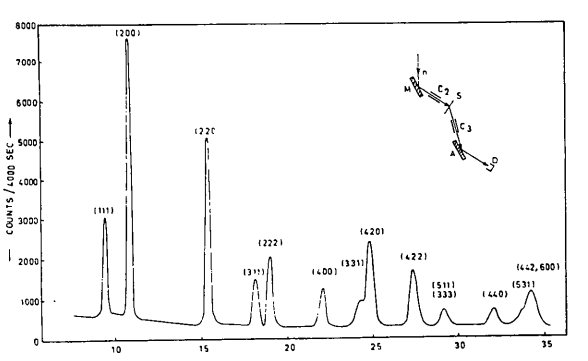

Fig. 4. Triple-axis neutron diffraction pattern of KCl powder.

$(1{\cdot}73 \pm 0{\cdot}21)$ Å^2. Comparing with the Mössbauer results (Butt & O'Connor, 1967) where the TDS correction is negligible, we estimate a sharply increasing (3 to 14%) TDS contribution to the Bragg peaks over the observed angular range.

The experiment was repeated in the triple-axis mode with a 2·5 meV energy resolution. The diffraction pattern thus obtained (Fig. 4) differs markedly from the double-axis pattern. In contrast to the double-axis pattern the background is decreasing with angle indicating a considerably reduced inelastic contribution. In this case the peaks are also better resolved. The B value obtained in the triple-axis case is $(2{\cdot}17 \pm 0{\cdot}15)$ Å^2, which agrees well with the TDS corrected values of other workers listed in Table 1.

Theory given in § 3 was used to calculate the relative TDS contamination under the peaks in the double-axis and triple-axis diffraction patterns. Results for 420 peaks are shown in Fig. 5. Fig. 6 gives the calculated TDS correction as a function of $\sin\theta/\lambda$ for the double-axis mode, and the triple-axis work with energy resolution 2·5 meV (present experiment) as well as with a finer triple-axis resolution of 0·86 meV. In our triple-axis experiment the TDS is reduced by a factor of two for the peak at the lowest angle and up to a factor of six for the higher-angle peaks. Thus the TDS correction varies slowly from $1\frac{1}{2}$ to 3% over the range of observation, and the error in the B value due to TDS is much smaller than the total experimental error and can be neglected. The experiment could not be performed with a better resolution because we did not have suitable monochromator and analyser crystals with smaller lattice constants for these experiments.

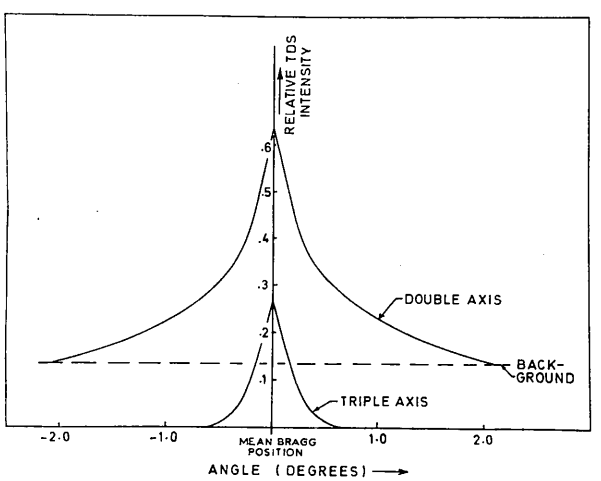

Fig. 5. Angular distribution of the relative TDS intensity under the Bragg peak is shown for the 420 reflexion of KCl. The observed base width in the double-axis case is 4·2° and in the triple-axis case is 2·3°.

5. Conclusions

Using the triple-axis neutron spectrometer the diffraction patterns have been obtained for KCl powder, in both the double-axis and the triple-axis modes. It is shown that in the triple-axis mode the TDS under the Bragg peaks is reduced to an extent that it can be neglected. The value of B thus obtained agrees well with TDS corrected results of other authors. Theoretical calculations are also presented which calculate the relative TDS correction for the two cases. The experimental results are supported by the results from these calculations.

It is a pleasure to thank Mr Ahmed Ali for his skilful technical assistance in operating the spectrometer. One of us (S.R.) is grateful to IAEA, AB Atomenergi, Sweden and Pakistan Atomic Energy Commission for financial support during his stay at PINSTECH.

APPENDIX

Derivation of the scattering surfaces for neutron scattering in the powder case

The basic equations for one phonon inelastic scattering are

$$\mathbf{K}_1 - \mathbf{K}_2 = \tau + \mathbf{q} \qquad (1)$$

Table 1. *Debye-Waller coefficient (B) of KCl*

No.	Method	Temperature (°K)	B_K(Å^2)		B_{Cl}(Å^2)	Reference
1	Mössbauer SC	290		2·19*		Butt & O'Connor (1967)
2	X-ray SC	290		1·885†		James & Brindley (1928)
3	X-ray P	300	2·08		2·06	Patomaki & Linkoaho (1968)
4	X-ray SC	298	2·15		2·15	Jayalakshmi & Viswamitra (1970)
5	Neutron P	295	2·00		2·08	Taylor & Willis (1973)
6	Neutron SC	295	2·175		2·165	Cooper & Rouse (1973)
7	Neutron P	300		2·17*		Present work
8	Theoretical	293	1·78		1·85	Copley *et al.* (1969)
9	Theoretical	295	1·929		1·995	Reid & Smith (1970)
10	Theoretical	290	1·91		1·73	Groenewegen & Huiszoon (1972)

* Average value for K and Cl ions.
† Value obtained by Nilsson (1957) after TDS correction to X-ray data of James & Brindley (1928).
Note: (i) The values quoted for Copley *et al.* have been obtained from their errata supplied with the reprint.
(ii) SC: Single Crystal: P Powder.

$$\frac{\hbar^2 K_1^2}{2m} - \frac{\hbar^2 K_2^2}{2m} = \pm \hbar\omega(\mathbf{q}) \tag{2}$$

where we have used the same notation as earlier.

To find the $\mathbf{q}$ value which satisfies the above equations we assume that $\mathbf{q} \ll \tau$; $\omega(\mathbf{q}) = c\mathbf{q}$ where c is the isotropic sound velocity of the material.

Setting

$$C = \frac{2m}{\hbar} c$$

we obtain from equation (2)

$$K_1^2 - K_2^2 = \pm Cq . \tag{3}$$

A coordinate system in the scattering plane of the reciprocal lattice is introduced with the x axis along the direction of τ, and we set

$$\tau = (x_0, 0); \quad \mathbf{q} = (x, y) . \tag{4}$$

For the double-axis case the wave vector of the incoming neutrons, $\mathbf{K}_1$, is fixed and the wave vector of the outgoing neutrons, $\mathbf{K}_2$, is fixed in direction but not in magnitude. This gives

$$\mathbf{K}_1 = (K_{1x}, K_{1y}) \tag{5}$$

$$\mathbf{K}_2 = [K_{2x}(1+t), K_{2y}(1+t)] . \tag{6}$$

Let the magnitudes of $\mathbf{K}_1$, and $\mathbf{K}_2$ be K and $K(1+t)$ respectively. By putting equations (4), (5) and (6) into equations (1) and (3) we obtain

$$K_{1x} - K_{2x}(1+t) = x_0 + x \tag{7}$$

$$K_{1y} - K_{2y}(1+t) = y \tag{8}$$

$$K^2 - K^2(1+t)^2 = \pm Cq . \tag{9}$$

Equations (7) and (8) give

$$\frac{K_{1x} - x_0 - x}{K_{1y} - y} = \frac{K_{2x}}{K_{2y}} \tag{10}$$

and equations (8) and (9) give

$$\frac{K^2}{C}\left[1 - \left(\frac{K_{1y} - y}{K_{2y}}\right)\right] = \pm q \tag{11}$$

where

$$q = (x^2 + y^2)^{-1/2} .$$

The scattering surface is the locus of the solution to equations (10) and (11). In the powder case, we have to rotate the $\mathbf{K}_1, \mathbf{K}_2$ configuration rigidly around the origin to obtain an average over all directions. Let the angle of rotation be φ (Fig. 1). For the scattering angle 2θ and an angle of rotation φ we obtain, assuming $\varphi \ll \theta$, as we are only interested in small q values,

$$K_{1x} = K(\sin\theta - \varphi\cos\theta) \tag{12}$$

$$K_{2x} = -K(\sin\theta + \varphi\cos\theta) \tag{13}$$

$$K_{1y} = K(\cos\theta + \varphi\sin\theta) \tag{14}$$

$$K_{2y} = K(\cos\theta - \varphi\sin\theta) . \tag{15}$$

Inserting the above expressions in equation (11) we obtain assuming $\varphi \tan\theta \ll 1$,

$$\frac{K^2}{C}\left[1 - \left(1 + 2\tan\theta - \frac{y(1+\varphi\tan\theta)}{K\cos\theta}\right)^2\right] = \pm q . \tag{16}$$

As $\varphi \ll 1, y \ll K$ the term proportional to $y\varphi/K$ is of second order and we can neglect it. We finally obtain

$$\frac{K^2}{C}\left(\frac{2y}{K\cos\theta} - 4\varphi\tan\theta\right) = \pm q . \tag{17}$$

Using equations (10) and (12) to (15) we get:

$$\varphi = \frac{x\cos\theta + y\sin\theta - \Delta\cos\theta}{x_0\sin\theta - y\cos\theta + x\sin\theta} \tag{18}$$

where

$$\Delta = 2K\sin\theta - x_0 . \tag{19}$$

At the exact Bragg position $\Delta = 0$ and we will assume $\Delta \ll x_0$.

By squaring both sides of equation (17) and putting the above value of φ we get:

$$\left(\frac{16}{x_0^2} - \frac{C^2}{K^4}\right) x^2 - \frac{C^2}{K^4} y^2 - \frac{32\Delta}{x_0^2} x + \frac{16\Delta^2}{x_0^2} = 0 , \tag{20}$$

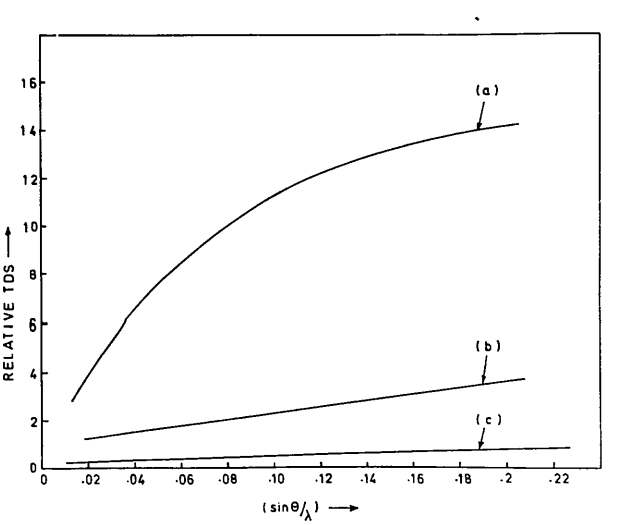

Fig. 6. Relative TDS contribution to the elastic peaks as a function of $(\sin\theta/\lambda)$ in: (*a*) Double-axis mode; (*b*) Triple-axis mode with energy resolution in this experiment (2·5 meV); (*c*) Triple-axis mode with energy resolution of 0·86 meV.

where we have used $2K\sin\theta\simeq x_0$ and assumed $x,y\ll x_0$.

By setting

$$d=\frac{C^2x_0^2}{16K^4}$$

equation (20) can be written

$$\frac{1-d}{d}\left(x-\frac{\Delta}{1-d}\right)^2-y^2-\frac{\Delta}{1-d}=0 \qquad (21)$$

which is the equation of the scattering surface in a plane. The scattering surface is cylindrically symmetrical around the reciprocal-lattice vector τ, and by using a cylindrical coordinate system (z,r,θ), with the z axis directed along τ we finally obtain the following equation for the scattering surface in reciprocal space

$$\frac{1-d}{d}\left(z-\frac{\Delta}{1-d}\right)^2-r^2-\frac{\Delta^2}{1-d}=0\,. \qquad (22)$$

References

BACON, G. E. (1962). *Neutron Diffraction*. Oxford: Clarendon Press.

BEG, M. M. & ROSS, D. K. (1968). *Neutron Inelastic Scattering*. Vol. II, pp. 299–312. Vienna: IAEA.

BUTT, N. M. & O'CONNOR, D. A. (1967). *Proc. Phys. Soc.* **90**, 247–252.

COOPER, J. M. & ROUSE, K. D. (1973). *Acta Cryst.* A**29**, 514–520.

COPLEY, J. R. D., MACPHERSON, R. W. & TIMUSK, T. (1969). *Phys. Rev.* **182**, 965–972.

GOMPF, F., LAU, H., REICHARDT, W. & SALGADO, J. (1972). *Neutron Inelastic Scattering*. pp. 137–147. Vienna: IAEA.

GROENEWEGEN, P. P. M. & HUISZOON, C. (1972). *Acta Cryst.* A**28**, 166–169.

JAMES, R. W. & BRINDLEY, G. W. (1928). *Proc. Roy. Soc.* A**122**, 155–171.

JAYALAKSHMI, K. & VISWAMITRA, M. A. (1970). *Phys. Lett.* **32**A, 83–84.

NILSSON, N. (1957). *Ark. Fys.* **12**, 247–257.

PATOMAKI, L. K. & LINKOAHO, M. V. (1969). *Acta Cryst.* A**25**, 304–305.

REID, J. S. & SMITH, T. (1970). *J. Phys. Chem. Solids*, **31**, 2689–2697.

ROY, A. P. & BROCKHOUSE, B. N. (1970). *Canad. J. Phys.* **48**, 1781–1788.

SEEGER, R. J. & TELLER, E. (1942). *Phys. Rev.* **62**, 37–40.

TAYLOR, R. I. & WILLIS, B. T. M. (1973). Private communication.

WILLIS, B. T. M. (1969). *Acta Cryst.* A**25**, 277–300.

WILLIS, B. T. M. (1973). *Chemical Applications of Thermal Neutron Scattering*. Oxford Univ. Press.

Acta Cryst. (1974). A**30**, 667

Coherent-Scattering Amplitude of ^{243}Am and ^{244}Cm*

BY M. H. MUELLER, G. H. LANDER AND J. F. REDDY

Materials Science Division, Argonne National Laboratory, Argonne, Illinois 60439, *U.S.A.*

(*Received* 18 *February* 1974; *accepted* 19 *April* 1974)

Neutron diffraction experiments have been completed on $^{243}AmO_2$ and $^{244}Cm_2O_3$. The coherent-scattering amplitude of ^{243}Am, relative to a value of $0{\cdot}58\times10^{-12}$ for oxygen, is $0{\cdot}76\ (1)\times10^{-12}$ cm. The value for curium is $\sim0{\cdot}7\times10^{-12}$ cm, which cannot be determined accurately in this experiment because both *C*-type (cubic, $a=11{\cdot}0$ Å) and *A*-type (hexagonal, isostructural with La_2O_3) Cm_2O_3 are present in the sample. Some of the difficulties in performing neutron diffraction experiments on these radioactive isotopes, which exhibit self-heating and spontaneous fission, are discussed briefly.

Introduction

Interest in the transuranium elements and their compounds has been almost totally confined, in the past, to nuclear physicists and chemists. Certainly, the structural chemistry of actinide compounds has been pursued vigorously, often on microgram quantities, since the early days of the Manhattan Project (Seaborg, 1958). The increasing availability of transuranium isotopes has meant, however, that experimentalists can now think in terms of gram rather than microgram quantities, and, over the last few years at Argonne National Laboratory (ANL) the electronic structure of a number of actinide compounds has been investigated with a variety of experimental techniques. Neutron diffraction plays an important role in these studies for two major reasons. First, the ordered arrangement of magnetic moments (many actinide compounds are magnetic at

* Work performed under the auspices of the U.S. Atomic Energy Commission.